表　注意欠陥/多動性障害の診断基準（DSM-IV）（文献1より引用）

A．(1)か(2)のどちらか：

(1) 以下の不注意の症状のうち6つ（またはそれ以上）が少なくとも6カ月以上続いたことがあり，その程度は不適応的で，発達の水準に相応しないもの：

不注意

(a) 学業，仕事，またはその他の活動において，しばしば綿密に注意することができない，または不注意な過ちをおかす．
(b) 課題または遊びの活動で注意を持続することがしばしば困難である．
(c) 直接話しかけられたときにしばしば聞いていないように見える．
(d) しばしば指示に従えず，学業，用事，または職場での義務をやり遂げることができない（反抗的な行動，または指示を理解できないためではなく）．
(e) 課題や活動を順序立てることがしばしば困難である．
(f) （学業や宿題のような）精神的努力の持続を要する課題に従事することをしばしば避ける，嫌う，またはいやいや行う．
(g) （例えばおもちゃ，学校の宿題，鉛筆，本，道具など）課題や活動に必要なものをしばしばなくす．
(h) しばしば外からの刺激によって容易に注意をそらされる．
(i) しばしば毎日の活動を忘れてしまう．

(2) 以下の多動性一衝動性の症状のうち6つ（またはそれ以上）が少なくとも6カ月以上持続したことがあり，その程度は不適応的で，発達水準の相応しない：

多動性

(a) しばしば手足をそわそわと動かし，またはいすの上でもじもじする．
(b) しばしば教室や，その他，座っていることを要求される状況で席を離れる．
(c) しばしば，不適切な状況で，余計に走り回ったり高い所へ上ったりする（青年または成人では落ち着かない感じの自覚のみに限られるかも知れない）．
(d) しばしば静かに遊んだり余暇活動につくことができない．
(e) しばしば“じっとしていない”または，まるで“エンジンで動かされるように”行動する．
(f) しばしばしゃべりすぎる．

衝動性

(g) しばしば質問が終わる前に出し抜けに答え始めてしまう．
(h) しばしば順番を待つことが困難である．
(i) しばしば他人を妨害し，邪魔する（例えば会話やゲームに干渉する）．

B．多動性一衝動性または不注意の症状のいくつかが7歳以前に存在し，障害を引き起こしている．

C．これらの症状による障害が2つ以上の状況において（例えば学校［または仕事］と家庭）存在する．

D．社会的，学業的または職業的機能において，臨床的に著しい障害が存在するという明確な証拠が存在しなければならない．

E．その症状は広汎性発達障害，精神分裂病，または，その他の精神病性障害の経過中にのみ起こるものではなく，他の精神疾患（例えば気分障害，不安障害，解離性障害，または人格障害）ではうまく説明されない．

▶病型に基づいてコード番号をつけること：

314.01　注意欠陥/多動性障害，混合型：
過去6カ月間A1とA2の基準をともに満たしている場合

314.00　注意欠陥/多動性障害，不注意優勢型：
過去6カ月間，基準A1を満たすが基準A2を満たさない場合

314.01　注意欠陥/多動性障害，多動性一衝動性優勢型：
過去6カ月間，基準A2を満たすが基準A1を満たさない場合

コード番号をつける上での注意：（特に青年および成人で）現在，基準を完全に満たさない症状を持つものには“部分寛解”と特定しておくべきである．

Age (yr)	Development of Mind	Symptoms of ADHD	Prefrontal Lobe Dysfunction
1	反応を抑制（遅延反応）	脱抑制	
	↓	↓	行動抑制（behavior
2～4	事実から感情を分離（情動を抑制：動機の形成）	衝動性	inhibition）の低下
	↓	↓	
	時間知覚（過去を思い出せ，未来を認識する：自己認識の形成）	非言語的表象能力低下 ソーシャルスキルの低下	
	↓	↓	作業記憶（working
5～6	内言語（言語で行動をコントロールできる：自由意思の根底）	言語的表象能力低下 セルフコントロールの低下	memory）の低下
	↓	↓	
7～	事実を分析し統合（世界を自分の中に取り込む：概念化）	プランニングの低下	実行機能（executive function）の低下

図　心の発達，ADHD の症状と前頭葉機能障害の関係

どの不安障害（約20%），抑うつなどの気分障害，適応障害などの併存障害が生じてくる。

このような ADHD の生物学的背景に起因した基本症状や一部の合併症と，社会生活や対人関係の悪循環の中で認められる併存障害は，同時期あるいは経時的に認められるため，ADHD の基本症状が隠されてしまうことが少なくはない。あくまで，治療の原則は ADHD の基本症状の改善を図ることなので，ADHD の基本症状を習熟しておきたい。

Ⅳ．小児科の役割

ADHD で最終的に問題となってくるのは，落ち着きのなさなど ADHD の基本症状や学習障害などではなく，二次性障害の中心である「心」の問題である。ADHD 児は周囲から理解されない存在として，我々が思っている以上に自己評価（self-esteem）が低い。したがって，自己評価を下げないため，基本症状のコントロール，安定した感情と学校生活を保障するための対応が必要になってくる。具体的な薬物療法，行動療法，環境変容法，家族・教師への対応，カウンセリング等は専門書に譲り，本稿では今までとは違った角度から ADHD の特性を小児科の先生方に知って頂くために，神経心理学的立場から ADHD を考えてみたい（図）。

神経心理学とは，知覚と認知，学習と記憶，言語・感情とコミュニケーション，理論と思考などの「心の神経メカニズム」のことである。従来から，神経心理学が人の脳損傷あるいは機能障害によって生じた症状から，神経学（脳）と心理学（心）を統合する役割を担ってきた。近年，ADHD を理解する神経心理学的理論として，Barkley によって提案された行動抑制（behavior inhibition）と実行機能（executive function）の障害が，ADHD の病態生理を考えるときの中心モデルとなってきた[14]。

発達の順序性からは，まず自己抑制が出現し，次に実行機能が順次認められてくる。生後数カ月から人は反応を遅らせる能力（遅延反応）が認められるようになる。これは，瞬時の情動（emotion）を抑制することである。もし，反応を抑制できなければ，短期的な報酬を求め，嫌なことから逃げ，間違った行動を繰り返し，さらに自分の思考を内・外

からの干渉から抑制できない。ADHD の基本症状は，自己抑制機能の発達障害と考えられる。

人は，このように外から入ってくる刺激に対して反応を遅らせることで，進化心理学的立場から長谷川が例えた「認知的贅沢」の恩恵を受けることが可能になる[15]。我々は行動を遂行する際，その行動が将来にどのような利益（報酬）をもたらすか，あるいは不利益（罰）を受けるか予想して行動を随時調節している。このような行動様式には，他者の行動や自分の過去の経験から学習し，将来の自己をイメージする非言語性作業記憶が必要とされる。近年，必要な情報を適切に選び（set），一時的に保持しつつ（short-term memory），不必要になったら消去する（reset）といった一連の情報処理過程すなわちワーキング・メモリー（working memory）が，前頭葉機能とくに認知・行動の時間的統合化（temporal integration）に関わっていることが提唱されている[16]。

この能力から，時間知覚が発達し，自己認識の形成からソーシャルスキルといったものが備わってくる。ADHD 児は，この将来のイメージを使えないため，未来に向かって意図した行動がとれず，現在の情動に依存した行動となる。5～6歳ごろより言語の内在化によって，言語を用いて思考し，行動を制御できる能力すなわち言語性作業記憶が発達する。その結果，自分自身に対し言語で指示できることで，セルフコントロールが可能となり，自由意思が形成される。また，情動も内在化するため，行動に直接結びつく怒り，恐れといった基本感情は複合化され，二次的な混合感情が意識されるようになる。このように情動が内在化された状況が，将来への動機（motivation）づけられた状態となっていく。ADHD 児は，これらの言語・情動の内在化が未熟なため，報酬がなくても自分自身を動機づけて継続的に作業することが困難になる。最後の実行機能は，カオスの状況にある外界の事実を，自己の中で分解，分析して再構築することで世界を自分の中に取り込むことができる能力である。この能力により，人は創造性を獲得する。

このように，人の心の発達を行動抑制と実行機能という視点からとらえると ADHD 児を理解しやすく，さらに脳（とくに前頭葉）機能障害として生物学的見地から捉えることが可能になると考えられる。

文　献

1) 米国精神医学会（高橋三郎，大野　裕，染谷俊幸，訳）：DSM-IV，精神疾患の分類・統計マニュアル，医学書院，東京，1996
2) Gjone H, Stevenon J, Sundet JM：Genetic influence on parent-reported attention-related problems in a Norwegian general population twin sample. J Am Acad Child Adolesc Psychiatry 35：588～596, 1996
3) Cook EH Jr, Stein MA, Krasowski MD et al：Association of attention deficit disorder and the dopamine transporter gene. Am J Hum Genet 56：993～998, 1995
4) LaHoste GJ, Swanson JM, Wigal SB et al：Dopamine D4 receptor gene polymorphism associated with attention deficit hyperactivity disorder. Mol Psychiatry 1：121～124, 1996
5) Amen DG, Carmichael BD：High-resolution brain SEPCT imaging in ADHD. Ann Clin Psychiatry 9：81～86, 1997
6) 安原昭博，吉田由香，堀あいこ：ADHD における No-Go Potential. 臨床脳波 45：755～758，2003
7) 稲垣真澄，白根聖子，加我牧子：AD/HD児の高次脳機能評価：視覚性弁別課題による検討. 臨床脳波 45：767～772，2003
8) 神谷裕子，相原正男，畠山和男他：能動的注意持続注意課題遂行時における意識変化の定量化に関する検討―体性感覚事象関連電位出現前後の脳波パワースペクトル解析―. 脳波と筋電図 27：371～379，1999
9) Aihara M, Aoyagi K, Goldberg E et al：Age shifts frontal cortical control in a cognitive bias task from right to left：part I. Neuropsychological study. Brain Dev 25：555～559, 2003
10) Shimoyama H, Aihara M, Fukuyama H et al：Context-dependent reasoning in a cognitive bias task：part II. SPECT activa-

tion study. Brain Dev 26：37～42, 2004
11) 神谷裕子，相原正男，長田美智子他：前頭葉機能の側性化に関する電気生理学的検討―Cognitive bias task 施行中の脳波周波数解析―．認知神経科学 3：188～191，2002
12) 山城 大，相原正男，小野智佳子他：併存障害のある注意欠陥/多動性障害児における交感神経皮膚反応の検討．脳と発達 36：49～54，2004
13) Damasio AR, Tranel D, Damasio H：Individuals with sociopathic behavior caused by frontal damage fail to respond autonomically to social stimuli. Behav Brain Res 41：81～94, 1990
14) ラッセル・A・バクーレー（原 仁訳）：ADHD の理論と診断―過去・現在・未来―．発達障害研究 24：357～376，2003
15) 長谷川寿一，長谷川眞理子：進化と人間行動．東京大学出版会，2000
16) Fuster MJ：The prefrontal cortex：anatomy, physiology, and neuropsychology of the frontal lobe. Lippincott - Raven, Philadelphia, New York, 2000

推薦図書

ADHD の解説書：ADHD のすべて．・ラッセル・A・バクーレー（海輪由香子，訳）・ヴォイス

前頭葉機能の解説書：The executive brain-frontal lobes and the civilized mind-・Goldberg E・Oxford

☆ ☆ ☆ ☆ ☆ ☆

鎮静薬—臨床検査における適正使用

金村英秋* Hideaki Kanemura
相原正男 Masao Aihara

Most Valuable Points

1）小児に安全な鎮静薬は抱水クロラールとトリクロフォスである。
2）追加投与により覚醒遅延などがみられるので，過量投与にならないよう注意する。
3）ベンゾジアゼピン系薬剤では，効果，安全性の点からダイアップ坐剤もしくはミダゾラムが推奨される。
4）小児患者に鎮静を行う際に重要なことは，どの鎮静薬を用いるかではなく，いかに安全に鎮静を行うかである。

I．鎮静にあたっての留意点

MRI検査をはじめとして，日常行う検査にあたって患者の協力を必要とする検査は少なくない。しかし，幼児以下の小児は協力性がなく，なんらかの鎮静，不動化が必要である。しかし，幼児以下の小児では成人と比較して上気道閉塞をきたしやすいうえに，呼吸器系のトラブルが多く，鎮静にあたってのリスクも大きい。このため，北米ではMRIなど，より深い鎮静を必要とする検査にあたっては小児麻酔科医が管理することが増えてきているが，日本では麻酔科医が不足していることもあり，ほとんどの場合で各科担当医によって行われているのが現状である。そのためにも，鎮静薬について小児科医が熟知しておくことが重要である。ただし，小児患者に鎮静を行う際に重要なことは，どの鎮静薬を用いるかではなく，いかに安全に鎮静を行うかである。このことを十分踏まえ，本稿では鎮静にあたっての注意・留意すべき点についてまず述べたうえで，鎮静薬の使用法および，小児の鎮静に用いられるそれぞれの薬剤に関して，その作用機序，有効性，副作用，安全性などについて述べる。

Key words：鎮静，呼吸抑制，気道閉塞
* 山梨大学医学部小児科
〔〒409-3898 山梨県中巨摩郡玉穂町下河東1110〕
TEL 055-273-9606 FAX 055-273-6745
E-mail：ykimu@yamanashi.ac.jp

II．鎮静にあたってのガイドライン

薬剤の選択は，一般に効果発現の速さと持続時間および安全性によりなされる。検査時の催眠には短時間作用型の鎮静薬がよいが，とくに安全性が要求されることは異論のないところである。しかし，Kaplanら[1]は，小児での鎮静時の危険性について検討し，薬剤の種類いかんにかかわらず，すべての種類の鎮静薬は推奨される量を用いたとしても問題を起こす可能性があることや，基礎疾患はなくとも1〜5歳の小児で最も危険性が高い点，合併症の原因で最もよく発生するのが，呼吸抑制，気道閉塞，無呼吸である点，合併症の発生頻度は多数の薬剤を併用（3剤以上）したときが高い点などを指摘している。このような危険性を十分考慮したうえで鎮静に当たる必要がある。米国小児科学会は1992年に鎮静のガイドラインを出している[2]。このガイドラインでは鎮静のレベルを示すとともに，小児患者に鎮静を行うときの重要な点について述べている。一方，米国麻酔科学会では，非麻酔科による鎮静・鎮痛時のガイドラインを1995年に初版を発表し，2002年に最新版に改訂した[3]。それには，15項目（患者評価，処置前準備，モニ

ター，モニターの記録，患者をモニターすべき人員，トレーニング，緊急用品の装備，酸素補助，鎮静薬と鎮痛薬との併用，鎮静・鎮痛薬の静脈投与，麻酔導入薬，静脈ライン，拮抗薬，回復室，サポート）にわたって，解説および推奨が示されている。これらは絶対的なものではないが，鎮静に際して小児科医として心得ておくべきである。

III．小児の鎮静に使用される主な薬剤

1．**抱水クロラール**（chloral hydrate，エスクレ® 坐剤 250・500 mg）

通常使用量：30～50 mg/kg（～75 mg/kg）

最大 1.5 g

比較的安全な睡眠薬，抗けいれん薬として小児科領域でも古くから用いられ，検査時の睡眠薬として頻用されている。粉末も存在するが，通常は坐剤を使用する。消化管からの吸収は速やかで，肝でアルコール脱水素酵素により trichloroethanol に分解され，これが抱水クロラールとともに中枢神経系に抑制的に働く。すなわち，投与直後の作用は抱水クロラールによるもので，その後の作用は trichloroethanol によるものとされている。坐剤の効果発現は数分後から 10 分前後であり，効果は 30 分から 1 時間以上続く。新生児はさらに長い。自然睡眠に近いという特徴があり，REM 睡眠は抑制しない。したがって，脳波や SPECT などの脳機能検査にも適している。呼吸への影響は基本的に少ないが，すでに上気道閉塞がある患者への投与は慎重を要する（可能であれば避けたほうがよい）。過量投与あるいは追加投与により覚醒遅延をきたすことがあり，さらに死亡例も報告されているので[4]，坐薬が排出された際の追加投与には注意が必要である。尿中へ排泄され，少量の代謝産物が便中へ排泄される。薬剤相互作用として，バルビタール系薬剤やフェノチアジン系薬剤などの作用を増強させることが知られている。また，アシドーシスや新生児高ビリルビン血症発現に注意を要する。その他の副作用としては，嘔吐，過敏症状（発疹，瘙痒感），興奮，多動がある。ポルフィリン症，ゼラチン過敏症では禁忌である。

2．**トリクロルエチルリン酸ナトリウム**（triclofos sodium，トリクロリール® シロップ）

通常使用量：20～80 mg/kg（～100 mg/kg）

最大 20 m*l*（2000 mg）

検査時の睡眠薬として頻用されている。生体内で trichloroethanol とリン酸に加水分解され，抱水クロラールと同様に trichloroethanol による睡眠作用を現す。したがって，効果，副作用ともに抱水クロラールとほとんど同じである。経口投与なので，作用発現時間は遅い。ポルフィリン症では禁忌である。

3．**ベンゾジアゼピン系薬剤**

神経細胞膜表面のγアミノ酪酸（GABA）受容体に作用して，神経細胞の活動を抑制する。そのため脳波，SPECT などでの検査には不適である。

1）**ジアゼパム**（diazepam，セルシン®，ダイアップ® 坐剤）

通常使用量：0.1～0.3 mg/kg（静注）

0.2～0.5 mg/kg（坐剤）

ライン確保の必要性がなく，副作用的にも安全な坐剤が使用しやすい。静注は血管痛があり，呼吸抑制をきたす場合がある。作用持続は比較的長く（2～6 時間），蓄積作用もある。効果発現は個体差が大きいために単独での使用は少ない。腸肝循環や肝臓での活性代謝産物（オキサゼパム）の生成により，投与 6～8 時間後に再鎮静が生じうる。肝機能障害がある患児では注意が必要である。新生児では半減期が長く，また保存料であるベンジルアルコールのビリルビン遊離作用が新生児黄疸を増悪させることがあるので，原則として使用しないほうがよい。坐薬と併用すると呼吸停止をきたしやすい。拮抗薬にはフルマゼニール（アネキセート®）がある。

2）**ミダゾラム**（midazolam，ドルミカム®）

通常使用量：0.025～0.15 mg/kg（静注）

作用時間は比較的短く（1～2 時間），調節性に富む。活性代謝産物もなく，遷延や蓄積の心配が少ない。また水溶性であるため，血管痛がなく，希釈しても白濁しない。麻薬と併用すると無呼吸を起こしやすい。

4．バルビツレート

中脳網様体賦活系などに作用し，鎮静・催眠から全身麻酔まで，中枢抑制のすべての段階に使用しうる。しかし，用量依存性の進行性中枢神経機能抑制作用を示す性質から呼吸抑制の危険性が高いこと，翌日への効果の持ち越し，精神機能の抑制などが問題としてあげられ，検査にあたっての鎮静としては慎重を要する。代表的なものとして以下の薬剤がある。

1）**ペントバルビタール**（pentobarbital）

通常量：0.5～1.0 mg/kg（静注）

作用時間は1～3時間と短い。

2）**チアミラール**（thyamylal），**チオペンタール**（thiopental）

通常量：1～5 mg/kg（静注）

作用時間は5～15分である。喘息患者には禁忌である。

5．抗ヒスタミン薬

ヒドロキシジン（hydroxyzine，アタラックスP®）

通常量：0.5～1.0 mg/kg（経口）

0.25～1.0 mg/kg（静注）

作用時間は経口で4～8時間，静注で1～4時間である。アジュバンド効果を有し，他の鎮静薬の効果を増強する。

6．**ケタミン**（ketamine，ケタラール®）

通常量：0.1～0.5 mg/kg（静注）

作用時間は5～15分である。鎮痛作用をもち，疼痛を伴う処置（骨髄穿刺など）における鎮静に有効である。しかし，副作用として脳圧亢進，気道口腔内分泌物の増加があげられ，副作用の点より検査目的での鎮静には適さない。NMDA受容体の非競合的拮抗が主な作用機序である。

7．**プロポフォール**（propofol）

通常量：1～3 mg/kg（静注）

非バルビタール静脈麻酔薬で深鎮静にも使用しうるが，呼吸抑制に対する対応が必須である。作用時間は5～10分と超短時間作用性であり，中止後のもうろう状態が少ないのが利点である。

ま と め

診断のために必要な検査であっても，患者のリスクを無視してまでも鎮静を行うという考えには異論を唱えるべきと考える。小児患者にいかに安全な医療を提供するか，その一環としてどのような鎮静を考えればよいかを常に念頭においた対応が望まれる。

文 献

1) Kaplan RF, Yang CI：Sedation and analgesia in pediatric patients for procedures outside the operating room. Anesthesiol Clin North America 20：181-193, 2002
2) American Academy of Pediatrics Committee on Drugs：Guidelines for monitoring and management of pediatric patients during and after sedation for diagnostic and therapeutic procedures. Pediatrics 89：1110-1115, 1992
3) An updated report by the American society of anesthesiologists task force on sedation and analgesia by non-anesthesiologists：Practice guidelines for sedation and analgesia by non-anesthesiologists. Anesthesiology 96：1004-1017, 2002
4) Jastak JT, Pallasch T：Death after chloral hydrate sedation：report of case. J Am Dent Assoc 116：345-348, 1988

*　　*　　*

ELSEVIER

Brain & Development 26 (2004) 37–42

BRAIN & DEVELOPMENT
Official Journal of the Japanese Society of Child Neurology

www.elsevier.com/locate/braindev

Original article

Context-dependent reasoning in a cognitive bias task Part II. SPECT activation study

Hitoshi Shimoyama[a], Masao Aihara[a,*], Hidenao Fukuyama[b], Kazuo Hashikawa[b], Kakurou Aoyagi[a], Elkhonon Goldberg[c], Shinpei Nakazawa[a]

[a]*Department of Pediatrics, Faculty of Medicine, University of Yamanashi, 1110 Tamaho-cho, Nakakomagun, Yamanashi 409-3898, Japan*
[b]*Department of Functional Brain Imaging, Human Brain Research Center, Graduate School of Medicine, Kyoto University, Kyoto, Japan*
[c]*Department of Neurology, New York University School of Medicine, New York, NY, USA*

Received 29 January 2003; received in revised form 14 April 2003; accepted 14 April 2003

Abstract

A cognitive bias task (CBT) delineates two different cognitive selection mechanisms in the prefrontal cortex. To identify functional anatomy of context-dependent reasoning, we used technetium-^{99m}hexamethyl- propyleneamine oxime (^{99m}Tc HM-PAO) single photon emission computed tomography (SPECT) and statistical parametric mapping. Twelve right-handed men 20–24 years old were instructed to look at a target card and then select the choice card (among two) that they preferred (modified CBT; mCBT). They also selected a choice card 2 weeks later without prior presentation of a target card (control task). In both tasks, ^{99m}Tc HM-PAO was injected intravenously about 15 s after initiation of the mCBT or control task. Brain images were obtained using a gamma camera and reconstructed by a UNIX-based workstation. Statistical analysis compared all activated images to control images. Results associated with P values of less than 0.01 (Z score >2.36) were depicted on T_1-weighted magnetic resonance images. All subjects preferred choices more similar to the target. SPECT activation occurred bilaterally in the dorsolateral prefrontal cortices and middle temporal gyri during performance of the CBT. Additionally, the left inferior prefrontal cortex and left fusiform gyrus showed significant activation compared with the control task. A neural network linking the temporal and prefrontal cortices prominently seen in the left hemisphere participates in context-dependent reasoning. Knowledge of such neural systems is essential for understanding prefrontal lobe function and dysfunction.

Keywords: Cognitive bias task; Context-dependent reasoning; Activation study; Single-photon emission computed tomography (SPECT); Statistical parametric mapping (SPM); Frontal lobe; Prefrontal lobe

1. Introduction

The prefrontal cortex has two cognitive selection mechanisms. One processing mechanism carries out exploratory processing of novel cognitive situations (context-independent reasoning), while the other carries out processing based on pre-existing representations (context-dependent reasoning) [1–3]. Goldberg et al. [4] recently described context-dependent and context-independent selection as respectively associated with the left and right frontal lobe, in right-handed male adults. Patients with left frontal lobe lesions showed context-independent reasoning in a cognitive bias task (CBT), while those with a right frontal lesion showed context-dependent reasoning. The shift accompanying routinization in the intact brain offers a dynamic view of lateralization of the frontal lobe. Aihara et al. have revealed that among right-handed male subjects, young children showed context-independent responses in a modified CBT (mCBT), while adolescents and adults showed context-dependent responses [5]. Thus, the locus of cortical control shifts from the right to the left frontal lobe as cognitive-contextual-reasoning develops. Accordingly, the CBT would be a highly informative cognitive activation task for imaging to lateralize function in the frontal lobes, providing a dynamic view of hemispheric specialization in terms of both laterality and region. However, the CBT has not been used in functional neuroimaging studies.

Functional neuroimaging has revealed much concerning brain function in perception and cognition [6,7]. At the same

* Corresponding author. Tel.: +81-55-273-9606; fax: +81-55-273-6745.
E-mail address: maihara@res.yamanashi-med.ac.jp (M. Aihara).

0387-7604/03/$ - see front matter © 2003 Elsevier B.V. All rights reserved.
PII: S0387-7604(03)00092-5

time, the frontal lobe has been implicated increasingly in developmental disturbances such as autistic disorder and attention deficit/hyperactivity disorder (ADHD) [8–10]. In this study we sought to identify the functional anatomy of context-dependent reasoning, using technetium-^{99m} hexamethyl-propyleneamine oxime (^{99m}Tc HM-PAO) single-photon emission computed tomography (SPECT) and statistical parametric mapping (SPM99).

2. Methods

2.1. Subjects

Twelve volunteers (all male; ages, 20–24 years) participated in this study. All subjects were right-handed [11], and had no history of psychiatric or neurologic illness. Informed consent was obtained from all subjects after the details of the study had been explained. The design of this study was approved by the ethical committee of the University of Yamanashi.

2.2. Task design

Goldberg et al. [4] proposed the CBT as a way to discriminate between left and right frontal lobe function. We used mCBT designed for children. The mCBT cards showed four characteristics: shape (circle or square), number (one or two), color (red or blue), and shading (unshaded outline or filled). At first one target card was presented. Two choice cards then were presented below the target card after 2 s. The subjects were instructed to look at the target card and then select a choice card according to their own preference. The 30 trial sequences that followed were the same for all subjects. As a control task, the subjects selected one of the two choice cards at random without prior presentation of a target card.

The mCBT raw score for each choice could range from 0 to 4 points. For example, if shape, color, and number but not shading were matched between the target card and the choice card, the raw score was 3 points. The overall mCBT raw score was the sum of similarity indices across trials, ranging from 30 to 90 points. High or low raw scores implied consistently similar choices (target-driven selection bias), while a middle-range score (around 60) implied that the choices were unrelated to the target (indifferent selection bias).

2.3. Imaging procedures

All subjects underwent both mCBT and control SPECT studies separated by an interval of 2 weeks. In both studies, technetium-^{99m} HM-PAO (370–740 MBq) was injected intravenously about 15 s after initiation of the mCBT or control task.

Brain images were obtained using a whole-body annular crystal gamma camera (Toshiba GCA-9300A/DI; Tokyo, Japan) equipped with low-energy, high-resolution three-head collimators. SPECT studies were acquired for 10 min in a 128 × 128 matrix with four degrees per second of continuous angular increment. These image reconstructions were performed at a UNIX-based workstation (Toshiba GMS-5500A Workstation; Tokyo, Japan).

2.4. Statistical parametric mapping

Analysis of data was performed by a personal computer with a Windows 2000 Professional Operating System using Statistical Parametric Mapping 99 software (SPM99; Institute of Neurology, University College of London, UK) [12]. The SPECT data reconstructed with attenuation and scatter collection were reformatted into the Analyze header format (Mayo Foundation, Baltimore, MD). SPECT images of each subject were co-registered between the activated and resting condition images. The data were then normalized to a high-resolution T1 template (Montreal Neurological Institution or MNI template) in lieu of our ^{99m}HM-PAO SPECT template to remove variation caused by differences in size and shape of individual brains, and smoothed with 8 mm full width at half maximum (FWHM) prior to SPM statistical analysis in order to improve statistical power by removing noise of the data. Statistical analysis was performed to compare all activated scans with all control scans. The results of t statistics were transformed to Z scores. The results were rendered on the reference T_1-weighted magnetic resonance images when P values were less than 0.01 (Z score, >2.36) with multiple comparison correction. For presentation, activated sections were rendered as hot-color maps on a three-dimensional surface view of the brain and also depicted on transverse slices.

3. Results

3.1. Behavioral data

All subjects performed the tasks well. Scores for each subject in the mCBT task exceeded 80 points (range, 82–90), which indicated that subjects responded in a highly context dependent-manner. The score for each subject in the control task was approximately 60 (range, 56–63), which reflected a context-independent mode of response.

3.2. SPECT activation data

CBT induced increased activation in a network system including right and left dorsolateral prefrontal cortices, right and left middle temporal areas, and the left insula and post-temporal area (Fig. 1). Exact locations as determined with Talairach coordinates are shown in Table 1.

Compared with the control task, CBT bilaterally

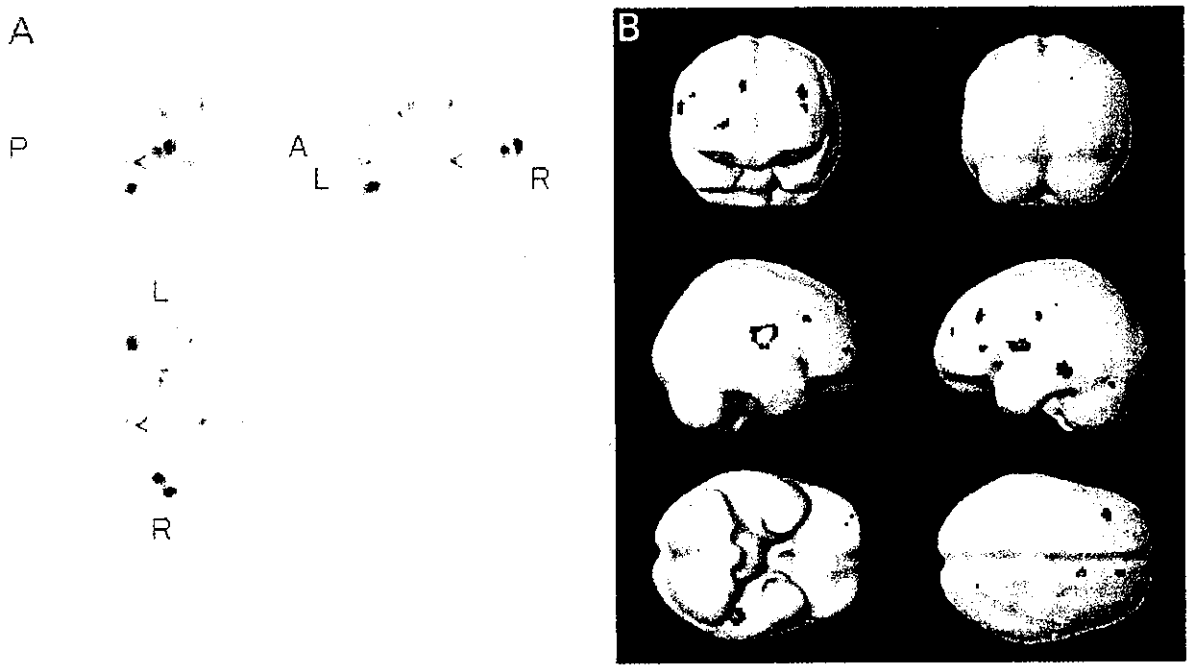

Fig. 1. Statistical parametric mapping (SPM). (A) Areas of significant activation ($P < 0.01$, corrected) are shown as a projection onto the glass brain. Coronal, viewed from behind; transverse, viewed from above; sagittal, viewed from right. (B) Surface SPM (Z) rendering images are superimposed upon three-dimensional magnetic resonance images. Activated regions are displayed in a 'hot' color.

activated the dorsolateral prefrontal cortices (BA 9/10/46) and the middle temporal gyri (BA 21/22); (Table 1; Fig. 2A,B). Activation also was significant in the left inferior prefrontal cortex (BA 45/47); (Table 1; Fig. 2B), the left premotor cortex (BA 6/24); (Table 1; Fig. 2C), and the left fusiform gyrus (BA 37); (Table 1; Fig. 2D).

4. Discussion

Traditional intelligence tests measure convergent thinking in the sense that a question usually has only one correct answer [13]. Tests of divergent thinking, in contrast, emphasize number and variety of answers to a single question. As CBT in our study requires divergent thinking, CBT was a multiple-choice response selection paradigm where preference rather than accuracy was examined. This mode of thinking has been reported to be particularly compromised by frontal lobe injury [13]. Performance of CBT by right-handed men with right prefrontal lesions showed an extreme response bias [4]. A group with left-sided lesions showed an opposite response bias. These findings suggest that left and right prefrontal systems exhibit different response selection biases: those guiding behavior according to internal context-based principles, and those using external environment-based principles [4]. In our mCBT study, all subjects preferred the choice most similar to the target. Therefore, we believe that our subjects selected one of the two choice cards based on internal context ordering hypothesized to involve the left prefrontal cortex in right-handed males.

Podell et al. [14] proposed that a CBT offers distinct advantages as a cognitive activation task for functional neuroimaging of the frontal lobes, since CBT discriminates well between the effects of left and right frontal lesions but still requires less time to administer, is easier to understand, and is better tolerated by subjects than the Wisconsin card sorting test (WCST), the current 'gold standard' for testing frontal lobe function. For functional neuroimaging, we chose a control task omitting presentation of a target card as an appropriate subtraction task for use with the CBT. This control task does not require the subject to make any 'most similar' or 'most different' choice. Operationally, the control task is identical to the CBT except for the presentation of the target card and subsequent divergent thinking, which are removed. With these task designs we could isolate response selection strategies and relate them to brain structures through SPECT activation imaging.

In this study the dorsolateral prefrontal cortices and middle temporal gyri were activated bilaterally as right-handed men performed the inherently ambiguous CBT. The left inferior prefrontal cortex and left fusiform gyrus also were significantly activated. Though clinical evidence has shown two functionally and neurally distinct cognitive selection biases [1,2], this study apparently is the first to show functional neuroimaging evidence of a neural system for context-dependent reasoning by healthy volunteers in a CBT.

According to CBT studies by Goldberg et al. [4,15],

Table 1
Areas showing activation

Location	Brodmann area	Talairach coordinates			Z-score
		x	y	z	
L. temporal lobe, middle temporal gyrus	21 22	−44	−35	−5	3.44
R. temporal lobe transverse temporal gyrus	41 42 21 22	51	−17	17	3.35
L. frontal lobe, precentral gyrus	6 24	−24	−12	41	2.97
L. frontal lobe, superior frontal gyrus	6	−46	−14	32	2.82
L. frontal lobe, superior frontal gyrus	10	−38	55	17	2.75
L. frontal lobe, middle frontal gyrus	10 46				
L. frontal lobe, inferior frontal gyrus	45 46 47	−44	29	6	2.7
L. frontal lobe, middle frontal gyrus	9	−36	34	28	2.69
L. frontal lobe, superior frontal gyrus	9				
R. frontal lobe, superior frontal gyrus	9	12	44	35	2.63
L. temporal lobe, fusiform gyrus	37	−51	−73	−17	2.58
R. frontal lobe, superior frontal gyrus	10	26	51	3	2.58
R. frontal lobe, middle frontal gyrus	10				
R. frontal lobe, middle frontal gyrus	46 9	53	23	26	2.47
R. frontal lobe, inferior frontal gyrus	9				
R. frontal lobe, middle frontal gyrus	10	34	56	1	2.35

lateralized prefrontal lesions in right-handed males differentially alter performance: right frontal lesions produce context-dependent responses, while left-sided lesions result in context-independent response. Whether there is a right-to-left shift of frontal advantage as the function of learning remains to be determined in this SPECT activation study. In our recent electrophysiologic study, however, the EEG spectral power increased in the gamma frequency bands (30–40 Hz) from the right to the left prefrontal regions as the CBT became familiar [16]. Recent investigations have reported that synchronization in the gamma band reflects a processing mode or working cortex [17,18]. In addition, this dual phenomenon was dramatically demonstrated by Gold et al. [19]. Using PET, they studied changes in blood flow patterns in the course of performing complex 'delayed alternating response' task. At the early learning stage the activation was greater in the right prefrontal regions than in the left. At the late stage the pattern was reversed: there was more activation in the left than right prefrontal regions [20]. Therefore, our results suggest that context-dependent reasoning in a CBT requires not only activation of both prefrontal lobes, but also dynamic changes of activation from the right to the left prefrontal lobes: the right prefrontal lobe (BA 9/10/46) is activated during the early portion of 30-CBT trials, followed in later trials by left prefrontal lobe (BA 9/10/46) activation associated with working memory. All subjects responded in an extremely context-dependent manner. These findings also support the hypothesis that the locus of cortical control shifts from right to left prefrontal over the course of cognitive skill development [15], as seen for cognitive contextual reasoning development [5]. Ongoing investigation of these issues in our laboratory includes analysis of transient shift-related signals in a CBT by using the temporal resolution of event-related functional magnetic resonance imaging method.

Our mCBT cards differed dichotomously in four respects: shape, color, number, and shading. Thus, subjects were required to discriminate 16 different visual objects as they preferred. In this respect, the CBT is a visual categorization task. In a previous investigation, Sigala and Logothetis examined neural mechanisms of categorization learning in macaque monkeys, finding that neural activity in

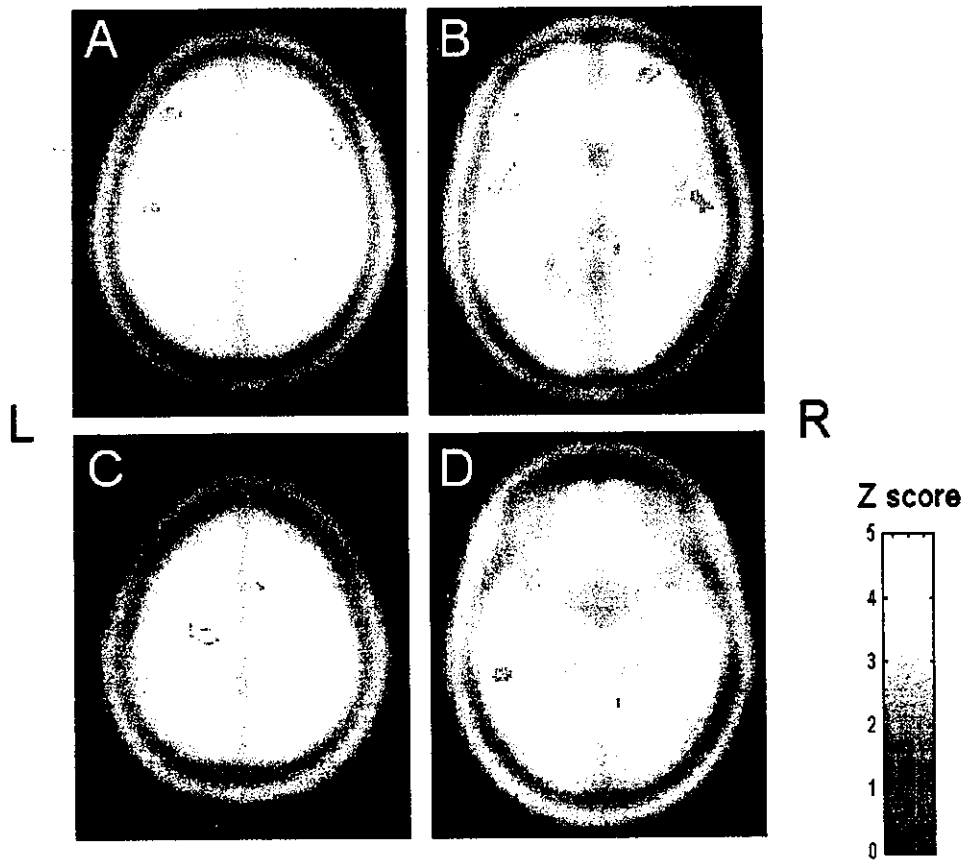

Fig. 2. Transverse statistical parametric mapping (Z) maps are superimposed upon magnetic resonance image. Coordinates are described with reference to the Talairach system. The local maximum within the activated volume is defined by the 'hot' color corresponding to (A) the left superior frontal gyrus ($x = -38$, $y = 55$, $z = 17$; $P < 0.01$, corrected; Z-score = 2.75); (A) the right superior frontal gyrus ($x = 26$, $y = 51$, $z = 3$; $P < 0.01$, corrected; Z-score = 2.58); (B) the left middle temporal gyrus ($x = -44$, $y = -35$, $z = -5$; $P < 0.01$, corrected; Z-score = 3.44); (B) the right transverse temporal gyrus ($x = 51$, $y = -17$, $z = 17$; $P < 0.01$, corrected; Z-score = 3.35); (C) the left middle frontal gyrus ($x = -24$, $y = -12$, $z = 41$; $P < 0.01$, corrected; Z-score = 2.97); and (D) the left fusiform gyrus ($x = -51$, $y = -73$, $z = -17$; $P < 0.01$, corrected; Z-score = 2.58).

the inferior temporal cortex was significantly enhanced during categorization in combined psychophysical and electrophysiologic experiments [21]. In humans, fine-grained categorization is selectively impaired after lesions that include the fusiform gyrus [22,23]. These findings indicate that activation of the temporal lobes, especially the fusiform gyrus, is critical for a visual categorization task such as CBT. Just after mCBT, on the other hand, all subjects had easy answering questions that probe the information of both target and choice cards presented lastly. In addition, it has been well known that the patients with damage to left fusiform gyrus are impaired at naming and retrieving information about visual objects [24,25]. These findings could provide an explanation why the left (not right) fusiform gyrus was activated by mCBT.

Prefrontal activation also has been correlated closely with a categorization task [26–28]. Hasegawa and Miyashita postulated that conceptual categorization is likely to depend on a neural network distributed between prefrontal and posterior association cortex, possibly including linguistic areas [22]. Activations in the left inferior prefrontal cortex (BA 45/47) and the left premotor cortex (BA 6/24) might be part of a language-related process in CBT. The present data indicate first that context-dependent reasoning in mCBT requires activation of a distributed network and second that the location of these sites are not symmetrically distributed, but rather prominently distributed in the left hemisphere, evidenced by the selective activation of the left fusiform, premotor and inferior frontal regions. Thus, context-dependent reasoning in mCBT would require activation of both retrieving visual information and internal speech [29,30]. Studies showing selective activation of left frontal cortex for naming and retrieving information about objects provide additional support for this view [29,31]. The likely mechanism can be inferred from our experiment that demonstrated reciprocal interactions between temporal and prefrontal cortices prominently seen in the left hemisphere along bottom-up and top-down connections in CBT including memory recall, retrieval [32–34], categorization [21], performance monitoring [35], decision making [36], and contextual updating [34].

5. Conclusion

Using ^{99m}HM-PAO SPECT and SPM99, we identified a neural network between temporal and prefrontal cortices prominently seen in the left hemisphere linked to context-dependent reasoning in mCBT. More detailed knowledge of such neural systems is essential for understanding frontal lobe function and dysfunction.

Acknowledgements

Our research was supported in part by The Japan Epilepsy Research Foundation (M.A.).

References

[1] Goldberg E, Costa LD. Hemispheric differences in the acquisition and use of descriptive systems. Brain Lang 1981;14:144–73.
[2] Lhermitte F. 'Utilization behavior' and its relation to lesions of the frontal lobes. Brain 1983;106:237–55.
[3] Milner B, Petrides M. Behavioural effects of frontal lobe lesions in man. Trends Neurosci 1984;7:403–7.
[4] Goldberg E, Podell K, Harner R, Riggio S, Lovell M. Cognitive bias, functional cortical geometry, and the frontal lobes: Laterality, sex, and handedness. J Cogn Neurosci 1994;6:276–96.
[5] Aihara M, Aoyagi K, Goldberg E, Nakazawa S. Age shifts frontal cortical control in a cognitive bias task from right to left: Part I. Neuropsychological study. Brain Dev 2003 doi: S0387-76 04(03)00064-0
[6] Caviness Jr VS, Lange NT, Makris N, Herbert MR, Kennedy DN. MRI-based brain volumetrics: emergence of a developmental brain science. Brain Dev 1999;21:289–95.
[7] Dong Y, Fukuyama H, Honda M, Okada T, Hanakawa T, Nakamura K, et al. Essential role of the right superior parietal cortex in Japanese kana mirror reading: An fMRI study. Brain 2000;123:790–9.
[8] Gorenstein EE, Mammato CA, Sandy JM. Performance of inattentive-overactive children on selected measures of prefrontal-type function. J Clin Psychol 1989;45:619–32.
[9] Swanson J, Castellanos FX, Murias M, LaHoste G, Kennedy J. Cognitive neuroscience of attention deficit hyperactivity disorder and hyperkinetic disorder. Curr Opin Neurobiol 1998;8:263–71.
[10] Happe F, Ehlers S, Fletcher P, Frith U, Johansson M, Gillberg C, et al. 'Theory of mind' in the brain. Evidence from a PET scan study of Asperger syndrome. Neuroreport 1996;8:197–201.
[11] Chapman LJ, Chapman JP. The measurement of handedness. Brain Cogn 1987;6:175–83.
[12] Nagayama Y, Fukuyama H, Yamauchi H, Matsuzaki S, Konishi J, Shibasaki H, et al. Cerebral activation during performance of a card sorting test. Brain 1996;119:1667–75.
[13] Milner B. Aspects of human frontal lobe function. In: Jasper HH, Riggio S, Goldman-Rakic PS, editors. Epilepsy and the functional anatomy of the frontal lobe. New York: Raven; 1995. p. 67–84.
[14] Podell K, Lovell M, Zimmerman M, Goldberg G. The cognitive bias task and lateralized frontal lobe functions in males. J Neuropsychiatry Clin Neurosci 1995;7:491–501.
[15] Goldberg E, Podell K. Lateralization in the frontal lobes. In: Jasper HH, Riggio S, Goldman-Rakic PS, editors. Epilepsy and the functional anatomy of the frontal lobe. New York: Raven; 1995. p. 85–96.
[16] Kamiya Y, Aihara M, Osada M, Ono C, Htakeyama K, et al. Electrophysiologic study of lateralization in the frontal lobes (in Japanese). Jpn J Cogn Neurosci 2002;3:188–91.
[17] Tallon-Baudry C, Bertrand O. Osillatory gamma activity in humans and its role in object representation. Trends Cogn Neurosci 1999;3: 151–62.
[18] Crone NE, Boatman D. Induced electrocorticographic gamma activity during auditory perception. Clin Neurophysiol 2001;112:565–82.
[19] Gold JM, Berman KF, Randolph C, Goldberg TE, Weinberger D. PET validation of a novel prefrontal task: delayed response alteration. Neuropsychology 1996;10:3–10.
[20] Goldberg E. The executive brain: frontal lobes and the civilized mind. New York: Oxford University Press; 2001.
[21] Sigala M, Logothetis NK. Visual categorization shapes feature selectivity in the primate temporal cortex. Nature 2002;415:318–20.
[22] Hasegawa I, Miyashita Y. Categorizing the world: expert neurons look into key features. Nat Neurosci 2002;5:90–1.
[23] Doran RJ, Fink GR, Rolls E, Booth M, Holmes A, Frackowiak RSJ, et al. How the brain learns to see objects and faces in an impoverished context. Nature 1997;389:596–9.
[24] Geschwind N, Fusillo M. Color-naming defects in association with alexia. Arch Neurol 1966;15:137–46.
[25] Damasio AR, Yamada T, Damasio H, Corbett J, McKee J. Central achromatopsia: behavioral, anatomic, and physiologic aspects. Neurology 1980;30:1064–71.
[26] Fuster JM. Executive frontal functions. Exp Brain Res 2000;133: 66–70.
[27] D'Esposito M, Ballard D, Zarahn E, Aguirre GK. The role of prefrontal cortex in sensory memory and motor preparation: An event-related fMRI study. Neuroimage 2000;11:400–8.
[28] Freedman DJ, Riesenhuber M, Poggio T, Miller EK. Categorical representation of visual stimuli in the primate prefrontal cortex. Science 2001;291:312–6.
[29] Grabowski TJ, Damasio H, Damasio AR. Premotor and prefrontal correlates of category-related lexical retrieval. Neuroimage 1998;7: 232–43.
[30] Gerlach C. Categorization and category effects in normal object recognition: a PET study. Neuropsychologia 2000;38:1693–703.
[31] Martin A, Wiggs CL, Ungerleider LG, Haxby JV. Neural correlates of category-specific knowledge. Nature 1996;379:649–52.
[32] Chao LL, Haxby JV, Martin A. Attribute-based neural substrates in temporal cortex for perceiving and knowing about objects. Nat Neurosci 1999;2:913–9.
[33] Buckner RL, Kelley WM, Petersen SE. Frontal cortex contributes to human memory formation. Nat Neurosci 1999;2:311–4.
[34] Shimamura AP. Memory retrieval and executive control process. In: Stuss DT, Robert TK, editors. Principles of frontal lobe function. London: Oxford University Press; 2002. p. 210–20.
[35] Gehring WJ, Knight RT. Prefrontal–cingulate interactions in action monitoring. Nat Neurosci 2000;3:516–20.
[36] Fuster JM. Overview of prefrontal functions: the temporal organization of behavior. The prefrontal cortex—anatomy, physiology and neuropsychology of the frontal lobe. 3rd ed. Philadelphia: Lippincott-Raven; 1997:209-252

ELSEVIER

Brain & Development 27 (2005) 148–151

BRAIN & DEVELOPMENT
Official Journal of the Japanese Society of Child Neurology

www.elsevier.com/locate/braindev

Original article

Sequential 3-D MRI frontal volume changes in subacute sclerosing panencephalitis

Hideaki Kanemura[a], Masao Aihara[a,*], Toshiyuki Okubo[b], Shinpei Nakazawa[a]

[a]*Department of Pediatrics, Faculty of Medicine, University of Yamanashi, 1110 Tamaho, Yamanashi 409-3898, Japan*
[b]*Department of Radiology, Faculty of Medicine, University of Yamanashi, 1110 Tamaho, Yamanashi 409-3898, Japan*

Received 26 November 2003; received in revised form 29 March 2004; accepted 9 May 2004

Abstract

In patients with subacute sclerosing panencephalitis, clinical stages defined according to Jabbour correlate strongly with frontal lobe dysfunctions. Nonquantitative radiologic investigations in these patients have confirmed cerebral atrophy without identifying predominantly affected regions. We addressed this issue over an 8-year-old boy's course using volumetry based on three-dimensional T1-weighted gradient echo magnetic resonance imaging. Seven normal 6–12-year-old subjects served as controls. Whole-brain volume declined as Jabbour stage advanced from I to III. Frontal lobe volume and frontal-to-whole-brain volume ratios fell significantly as clinical stage progressed. Thus, cerebral atrophy in this SSPE patient was predominantly frontal, and paralleled clinical progression.

Keywords: Subacute sclerosing panencephalitis (SSPE); Three-dimensional magnetic resonance imaging; Brain volumetry; Frontal lobe atrophy; Jabbour clinical stage

1. Introduction

Subacute sclerosing panencephalitis (SSPE), a rare, progressive, and frequently fatal infectious nervous system disease that affects children and young adults, is caused by an aberrant response to measles infection [1]. SSPE commonly is characterized by insidious onset of behavioral changes, emotional instability, and mental deterioration, followed by ataxia, myoclonic jerks, and focal neurologic signs [2]. A multidisciplinary study by Jabbour and coworkers [3] suggested a four-stage clinical classification that is used to evaluate disease progression. Clinical signs of SSPE such as emotional instability, behavioral changes, motor disturbances and myoclonic jerks correlate strongly with frontal lobe dysfunction.

Radiologic investigations using computed tomography (CT) and magnetic resonance imaging (MRI) in patients with SSPE confirmed cerebral atrophy [4,5], which is diffuse in the final stages of the disease [6]. However, the regions most severely involved were not identified in these qualitative studies.

We encountered a patient with SSPE who showed disturbance of motor function, lack of spontaneity, and emotional instability in his course. Marked improvement concerning emotional state and spontaneity occurred with long-term combined therapy with oral isoprinosine and intrathecal α-interferon. We serially measured total and frontal cerebral volumes by three-dimensional (3-D) MRI-based volumetry, correlating cerebral atrophy with clinical and laboratory data over time.

2. Case report

An 8-year-old boy was admitted to our hospital in November 1999 for evaluation of gait disturbance, dysarthria, and myoclonic jerks of the right upper limb. The second child of nonconsanguinous parents, he was born after an uneventful pregnancy and delivery and had normal motor and mental development up to the age of 8 years. Whether he had been infected with measles was unknown, but he had not received measles vaccine.

He showed lack of spontaneity and emotional instability. On neurologic examination he had myoclonic jerks of the right upper limb. Cranial nerve function was unremarkable.

* Corresponding author. Tel.: +81-55-273-9606; fax: +81-55-273-6745.
E-mail address: maihara@res.yamanashi-med.ac.jp (M. Aihara).

0387-7604/$ - see front matter © 2004 Elsevier B.V. All rights reserved.
doi:10.1016/j.braindev.2004.05.001

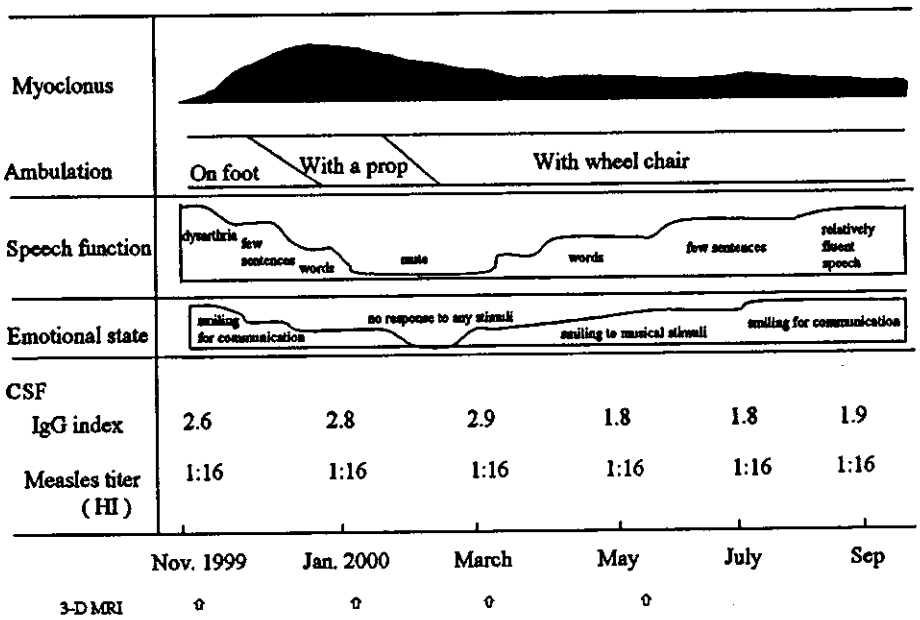

Fig. 1. Clinical course of a patient with SSPE. Symptoms rapidly progressed from Jabbour stage I to III, but improved to stage II by 6 months after initiating combination therapy. Measles titers in serum and cerebrospinal fluid showed no significant change throughout the course, but the IgG index changed in parallel with the clinical state. SSPE, subacute sclerosing panencephalitis; HI, hemagglutination inhibition.

Cogwheel rigidity was noted in the right limbs, where deep tendon reflexes were brisk. Results of routine hematologic and blood chemistry tests and urinalysis were normal. High measles antibody titers were found in serum (1:256) and cerebrospinal fluid (1:16). IgG was significantly elevated in the cerebrospinal fluid, as was the IgG index. Oligoclonal IgG bands were present in the cerebrospinal fluid. An electroencephalogram revealed periodic high-amplitude sharp- and slow-wave complexes. High-signal lesions were seen in the right parietal and occipital lobes on T2-weighted images. The patient was diagnosed with SSPE, and treatment was initiated immediately with combined oral isoprinosine and intrathecal α-interferon.

The patient's clinical course is shown in Fig. 1. He showed rapid progression from Jabbour stage I to III, followed by slow improvement from stage III to II. Initially ambulating unaided, he was wheelchair-bound or bedridden 2 months after onset of symptoms. He had not regained speech or responsiveness to stimuli at 3 months after initiation of therapy, and the Jabbour stage remained III. He regained responsiveness to stimuli and some speech 6 months after beginning combination therapy. Myoclonic jerks decreased in frequency, and emotional state was stable; improvement represented clinical stage II. Ambulation did not improve despite medical therapy and rehabilitation. Measles titers in cerebrospinal fluid showed no change throughout the course. On the other hand, the IgG index had changed from 2.6 at onset to 2.9 4 months later in association with clinical disease progression, but was 1.8 in association with clinical improvement at 6 months after onset. Routine MRI showed mild progression of brain atrophy and high signal intensity in subcortical white matter.

3. Serial 3-D MRI volumetry

Volumetric 3-D MRI evaluation was performed in the patient four times, at onset of symptoms and 2, 4, and 6 months after onset (Fig. 1).

A control group consisted of seven age-matched children, including five boys and two girls who ranged in age from 7 to 12 years (mean 9). Clinical indications for MRI included suspected speech delay, brain trauma, brain tumor, short stature, and migraine. No neurologic, cognitive, or emotional disorder was present in controls during 2–4 years of subsequent follow-up. No control subject had abnormal findings by routine MRI.

MRI was performed using a 1.5-Tesla system (GE, location). The 3-D MRI data were acquired by fast spoiled gradient recalled echo in a steady state with 3-D Fourier transformation. Images of the entire brain surface in 3-D were obtained from the 124 sections using an Advantage Windows RP 3-D analyzer (General Electric, Wisconsin, MW). Then frontal lobe was determined and confirmed using the same method as our previous report [7]. Finally we measured whole-brain and frontal lobe volumes using the volume measurement function of the analyzer workstation, based on the 3-D images.

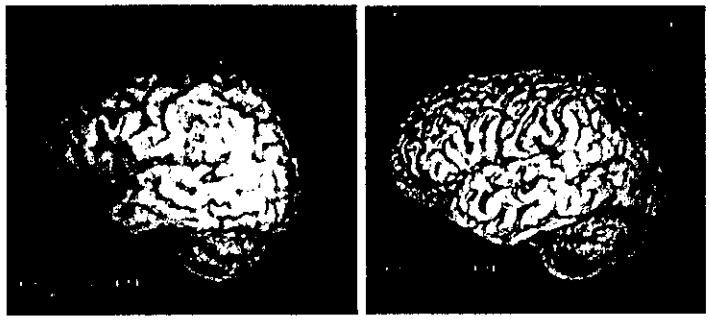

Fig. 2. Three-dimensional surface views of the left hemisphere 4 months after onset in a patient with SSPE (A) and in an age-matched normal control (B). SSPE, subacute sclerosing panencephalitis.

Fig. 2A depicts 3-D surface views of the patient's left hemisphere in comparison to those of a normal subject (Fig. 2B). The patient's frontal lobe was clearly atrophic to simple inspection. Serial MRI findings revealed increased signal on T2-weighted images in subcortical white matter, enlargement of lateral ventricles, and slowly progressive cerebral atrophy.

Measured volumes for whole brain and frontal lobe, and ratios of frontal lobe to whole-brain volume are shown in Fig. 3. Whole-brain volumes declined with progression of Jabbour stages from I to III remaining essentially unchanged thereafter during clinical improvement from stage III to II (Fig. 3A). Frontal lobe volume declined significantly with progression of clinical stage, then remaining constant (Fig. 3B). The frontal lobe to whole-brain volume ratio fell significantly with progression of clinical stage, and restored slightly during clinical improvement (Fig. 3C).

4. Discussion

Quantitation of volume is useful in characterizing normal brain growth as well as disturbances of growth caused by various diseases. Volumetric analysis of the brain may predict functions associated with the region measured. Using volumetry based on 3-D MRI, we investigated frontal and prefrontal normal growth during childhood and adolescence [7]. Reliability of MRI-based volumetric analysis reflects both image quality and the power of the analysis [8], as confirmed by comparison of direct and MRI volumetric measurements in cadaver brains. Furthermore, intra- and inter-rater variations were comparable to those in other studies [9].

Neuroimaging in the patients with SSPE is not absolutely required for diagnosis, but it offers important clues for clinical assessment. Reported distributions of MRI

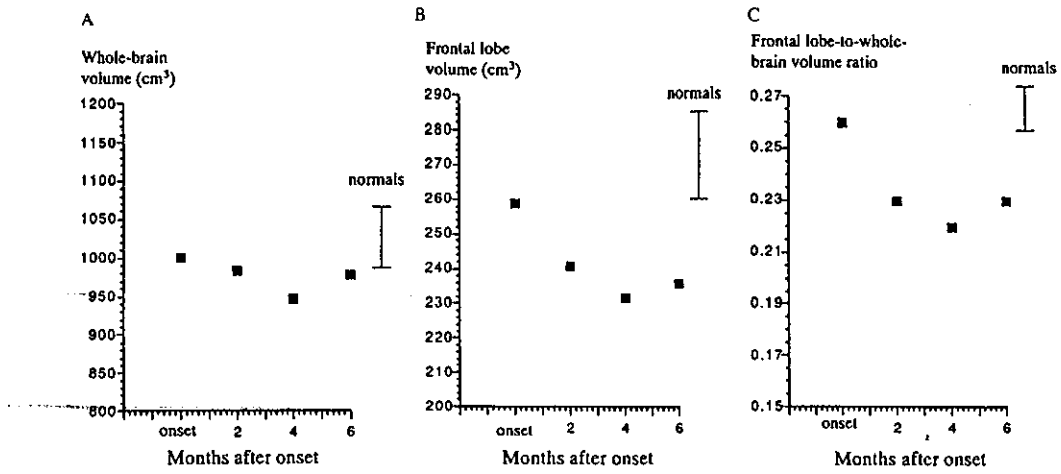

Fig. 3. Serial changes of whole brain volume (A), frontal lobe volume (B), and the frontal lobe to whole-brain volume ratio (C). Whole-brain volumes declined with progression of clinical stage according to Jabbour. Frontal lobe volume and the frontal lobe-to-whole-brain volume ratio also declined significantly with progression of clinical stage. Bars indicate the range for age-matched control patients who proved to have no neurologic disease.

abnormalities have varied between series [6,10,11]. Kulczycki et al. [12] found the inflammatory process to begin in occipital white matter and proceed toward the frontal region. As the disease progresses, lesions showing demyelination, necrosis, gliosis, and cerebral atrophy become increasingly prominent [10], as is best appreciated in T2-weighted images. However, correlations between clinical state and MRI findings have not been clear in previous reports [4,6,10]. Previous MRI studies performed at different stages of the disease [1,4,10,13,14] have suggested that SSPE can involve cortical gray matter, white matter, and basal ganglia, leading to atrophy. In previous reports mild atrophy was seen as early as 6 months, with subsequent progression [1]. In other reports, cerebral atrophy was observed in patients with a rapid disease course or an advanced disease stage [14]. Atrophy appears to result from postinflammatory tissue damage, and may occur earlier in patients with a relatively rapid course. Thus, the pattern of cerebral atrophy in a patient with SSPE can vary with clinical stage and duration of symptoms.

Symptoms of SSPE characteristically include an insidious onset of behavioral changes and emotional instability. Patients with frontal lesions also demonstrate a range of social impairments related to changes in personality and irresponsibility. Previous investigations have underscored the importance of the frontal cortex, especially the orbitofrontal cortex, in social interactions and emotional responses. On the basis of PET studies in SSPE, Huber et al. [15,16] hypothesized that inflammation associated with excessive metabolism in the basal ganglia interferes with connections between frontal, temporal, and parietal areas, resulting in Jabbour stage II symptoms. On the other hand, PET findings included decreased cerebral blood flow and oxygen metabolism in the frontal lobes [17], suggesting that frontal lobe function had a particularly strong correlation with clinical stage in SSPE.

To the best of our knowledge, no attempt has been made to measure individual cerebral lobes in patients with SSPE. Our study therefore may be the first to quantitate atrophy of the whole brain and frontal lobes in a patient with SSPE. Frontal lobe volumes, especially when considered as a ratio to whole-brain volume, decreased in association with advances of clinical stage and increases of the IgG index, and restored slightly with clinical improvements. Thus, cerebral atrophy in SSPE, particularly frontal lobe atrophy, might correlate with clinical and laboratory progression and improvement.

Clinical stage did not significantly reflect MRI findings when a heterogeneous group of SSPE patients was considered, although imaging findings correlated with clinical stage during the first year after onset [5]. Furthermore, serial MRI and clinical examinations carried out by Akdal et al. [18] exhibited little correlation between MRI findings and clinical stage. However, our patient showed a close relationship over time between frontal lobe atrophy and both the clinical state and the IgG index. Our investigation is the first to use quantitative and regional analysis based on 3-D MRI. In the future, investigations of the frontal lobe by serial 3-D MRI may have important role in clinical evaluation in SSPE.

In conclusion, our findings suggested that cerebral atrophy in a patient with SSPE occurred mainly in the frontal lobes and this technology may be a useful tool for understanding clinical dysfunctions of SSPE.

References

[1] Zeman W. Subacute sclerosing panencephalitis and paramyxovirus infections. In: Vinken PJ, Bryun GW, editors. Handbook of clinical neurology. Amsterdam: Elsevier; 1978. p. 343–68.

[2] Dyken PR. Subacute sclerosing panencephalitis. Neurol Clin 1985;3: 179–96.

[3] Ohya T, Martinez AJ, Jabbour JT, Lemmi H, Duenas DA. Subacute sclerosing panencephalitis. Correlation of clinical, neurophysiologic and neuropathologic findings. Neurology 1974;24:211–7.

[4] Brismar J, Gascon GG, Steyern KV, Bohlega S. Subacute sclerosing panencephalitis: evaluation with CT and MR. Am J Neuroradiol 1996; 17:761–72.

[5] Tuncay R, Akman-Demir G, Gokyigit A, Eraksoy M, Barlas M, Tolun R, et al. MRI in subacute sclerosing panencephalitis. Neuroradiology 1996;38:636–40.

[6] Anlar B, Saatci I, Kose G, Yalaz K. MRI findings in subacute sclerosing panencephalitis. Neurology 1996;47:1278–83.

[7] Kanemura H, Aihara M, Aoki S, Araki T, Nakazawa S. Development of the prefrontal lobe in infants and children: a three-dimensional magnetic resonance volumetric study. Brain Dev 2003;25:195–9.

[8] Caviness Jr. VS, Lange NT, Makris N, Herbert MR, Kennedy DN. MRI-based brain volumetrics: emergence of a developmental brain science. Brain Dev 1999;21:289–95.

[9] Aylward EH, Augustine A, Li Q, Barta PE, Pearlson GD. Measurement of frontal lobe volume on magnetic resonance imaging scans. Psychiatry Res 1997;75:23–30.

[10] Geller TJ, Vern BA, Sarwar M. Focal MRI findings in early SSPE. Pediatr Neurol 1987;3:310–2.

[11] Winer JB, Pires M, Kermode A, Ginsberg L, Rossor M. Resolving MRI abnormalities with progression of subacute sclerosing panencephalitis. Neuroradiology 1991;33:178–80.

[12] Kulczycki J, Kryst-Widzgowska T, Sobczyck W, Milewska D, Bochynska A. NMR and CT images in subacute sclerosing panencephalitis. Neurol Neurochir Pol 1994;28(suppl 1):79–90.

[13] Tsuchiya K, Yamauchi T, Fururi S, Suda Y, Takenaka E. MR imaging vs. CT in subacute sclerosing panencephalitis. Am J Neuroradiol 1988;9:943–6.

[14] Bohlega S, Al-Kawi MZ. Subacute sclerosing panencephalitis: imaging and clinical correlation. J Neuroimaging 1994;4:71–6.

[15] Huber M, Herholz K, Pawlik G, Szelies B, Jurgens R, Heiss W-D. Cerebral glucose metabolism in the course of subacute sclerosing panencephalitis. Arch Neurol 1989;46:97–100.

[16] Huber M, Pawlik G, Bamborschke S, Fink GR, Karbe H, Schlenker M, et al. Changing pattern of glucose metabolism during the course of subacute sclerosing panencephalitis as measured with ^{18}FDG-positron-emission tomography. J Neurol 1992;239:157–61.

[17] Yoshikawa H, Fueki N, Yoneyama H, Ogawa M, Sakuragawa N. Positron emission tomography demonstrated localized luxury perfusion in subacute sclerosing panencephalitis. J Child Neurol 1990;5: 311–5.

[18] Akdal G, Baklan B, Cakmakci H, Kovanlikaya A. MRI follow-up of basal ganglia involvement in subacute sclerosing panencephalitis. Pediatr Neurol 2001;24:393–5.

Case Report

Pediatric Neurosurgery

Pediatr Neurosurg 2004;40:230–233
DOI: 10.1159/000082297

Received: February 24, 2004
Accepted after revision: May 28, 2004

Intracranial Ectopic Recurrence of Craniopharyngioma after Ommaya Reservoir Implantation

Keisuke Ishii[a] Kenji Sugita[a] Hidenori Kobayashi[a] Tohru Kamida[a]
Minoru Fujiki[a] Tatsuro Izumi[b] Teruaki Mori[c]

Departments of [a]Neurosurgery and [b]Pediatrics, Oita University Faculty of Medicine, and
[c]Department of Neurosurgery, National Nishibeppu Hospital, Oita, Japan

Key Words
Craniopharyngioma · Total removal · Ectopic recurrence · Childhood · Ommaya reservoir

Abstract
We present a very rare case of a craniopharyngioma showing intracranial ectopic recurrence after the total removal of recurrent craniopharyngioma arising at the primary site accompanied by Ommaya reservoir implantation. A 2-year-old boy underwent a bifrontal craniotomy and total removal of the adamantinomatous craniopharyngioma via the interhemispheric translamina terminalis approach. Four months later, he underwent total removal of recurrent craniopharyngioma and implantation of an Ommaya reservoir via the same approach. Ten months later, total removal of the ectopic recurrent craniopharyngioma following the placement of the Ommaya reservoir cannula, which was placed within the surgical route, was performed via the same craniotomy.

Introduction

Craniopharyngioma is a benign neoplasm that accounts for approximately 2–3% of all intracranial tumors and arises from the squamous epithelial nests of Rathke's pouch [1–3]. Complete tumor excision is difficult due to the peripheral structure. The recurrence of craniopharyngioma is not rare and often occurs at the primary site or in an adjacent area. However, the ectopic recurrence of craniopharyngioma is very rare, and to date, only 12 cases have been reported [4–15]. The authors present a case of craniopharyngioma showing intracranial ectopic recurrence after the total removal of recurrent craniopharyngioma arising at the primary site.

Case Report

A 2-year-old boy presented at the Pediatrics Department of his local hospital on April 5, 2000, with headache, nausea and lethargy persisting since the middle of March 2000. Computed tomography (CT) demonstrated a suprasellar mass extending to the third ventricle and acute hydrocephalus. The patient was referred to our hospital and was admitted the same day. No remarkable abnormal neurological findings were detected. On magnetic resonance imaging (MRI), the mass measured 2.0 × 2.0 × 4.0 cm, with both solid and cystic components (fig. 1). The solid component was heterogeneously enhanced and included calcification. The cyst wall was well enhanced.

KARGER
Fax + 41 61 306 12 34
E-Mail karger@karger.ch
www.karger.com

1016–2291/04/0405–0230$21.00/0

Accessible online at:
www.karger.com/pne

Keisuke Ishii, MD, PhD
Department of Neurosurgery, Oita University Faculty of Medicine
1-1 Idaigaoka, Hasama-machi
Oita 879-5593 (Japan)
Tel. +81 97 586 5862, Fax +81 97 586 5869, E-Mail keisuke@med.oita-u.ac.jp

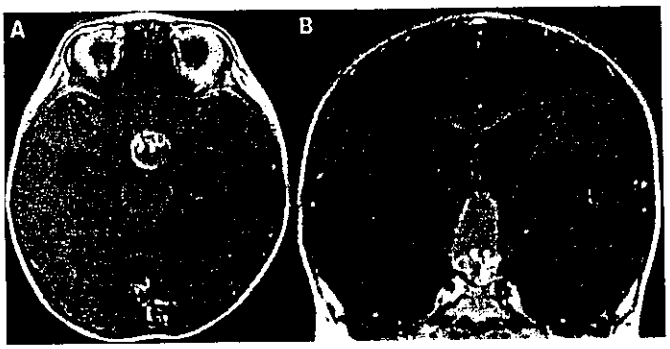

Fig. 1. Axial T_1-weighted gadolinium-enhanced (**A**) and coronal (**B**) MR images demonstrated a well-enhanced suprasellar mass extending to the third ventricle, and acute hydrocephalus. The mass measured 2.0 × 2.0 × 4.0 cm, with both solid and cystic components. The solid component was heterogeneously enhanced and included calcification. The cyst wall was well enhanced.

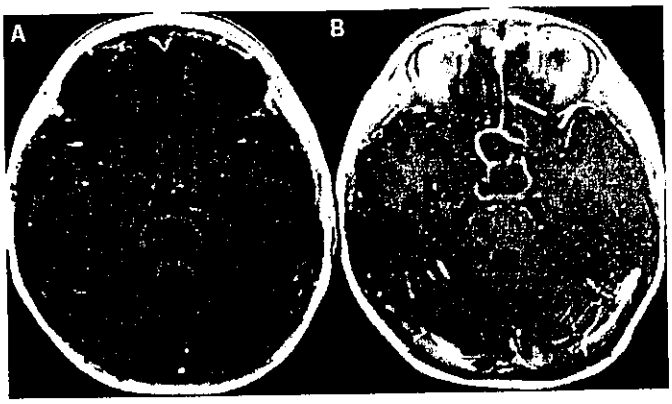

Fig. 3. Axial T_1-weighted gadolinium-enhanced MR images (**A**), 20 days after the initial surgery, revealed no residual tumor. Axial T_1-weighted gadolinium-enhanced MR images (**B**), 4 months after the initial surgery, revealed a recurrent tumor at the primary site and a trail of enhancement along the initial surgical tract (white arrow). This multilocular cystic mass measured 3.0 × 3.0 × 3.0 cm.

Fig. 2. Photomicrograph indicating a typical craniopharyngioma of the adamantinomatous type. Stratified squamous epithelium surrounding a loose 'reticulate' hypocellular region with multiple cysts and calcifications can be seen. HE. ×200.

Acute hydrocephalus was demonstrated, causing a mass on the third ventricle. We diagnosed craniopharyngioma and performed a bifrontal craniotomy with total removal of the tumor via the interhemispheric translamina terminalis approach on April 11. Histopathological examination confirmed the diagnosis of an adamantinomatous craniopharyngioma (fig. 2). MRI, 20 days after the first operation, revealed no residual tumor (fig. 3A). Postoperatively, the patient developed panhypopituitarism and diabetes insipidus. Thyroid hormone, an adrenal cortical hormone and an antidiuretic hormone were administered. No postoperative radiotherapy was administered. The patient was discharged without neurological deficits. Four months later, on August 28, the patient's mother noticed signs of visual impairment in her child. There had been no previous signs of visual impairment and he had not complained of this symptom until that time. He was extremely nearsighted, able to see only about 30 cm. MRI demonstrated recurrent suprasellar craniopharyngioma, a multilocular cystic mass measuring 3.0 × 3.0 × 3.0 cm (fig. 3B). The patient underwent total removal of the recurrent craniopharyngioma via the same approach. At this time, an Ommaya reservoir was implanted and the tip of the cannula was inserted into the extraction cavity for the management of future recurrence, for aspiration of the cystic component and reduction of the tumor mass. The histopathological examination was similar to that previously performed. Postoperatively, his visual impairment improved by degrees. However, CT on the sixth postoperative day demonstrated minute calcifications around the Ommaya reservoir cannula that had not been seen the day after surgery (fig. 4A, B). MRI after about 2 months demonstrated a cystic mass surrounding the Ommaya reservoir cannula in the center of the frontal base in the subdural space under the craniotomy bone flap (fig. 4C). After 6 months, CT revealed an enlarged well-enhanced cystic mass involving minute calcifications around the cannula (fig. 4D). On June 26, 2001, 10 months after the previous operation, total removal of the tumor was performed via the same craniotomy since this cystic lesion had grown gradually (fig. 5). The Ommaya reservoir cannula was removed from the recurrent tumor during the surgical procedure. There was no adherent tumor tissue, including calcification, and the histopathological features of the tumor were identical to those of the adamantinomatous craniopharyngioma that had been removed previously. There was no evidence of histological malignancy such as nuclear atypia, high mitotic activity or necrosis. The postoperative clinical course was good with no neurological deficits. Routine follow-up MRI 2 years and 7 months after the third operation revealed no evidence of recurrent tumor.

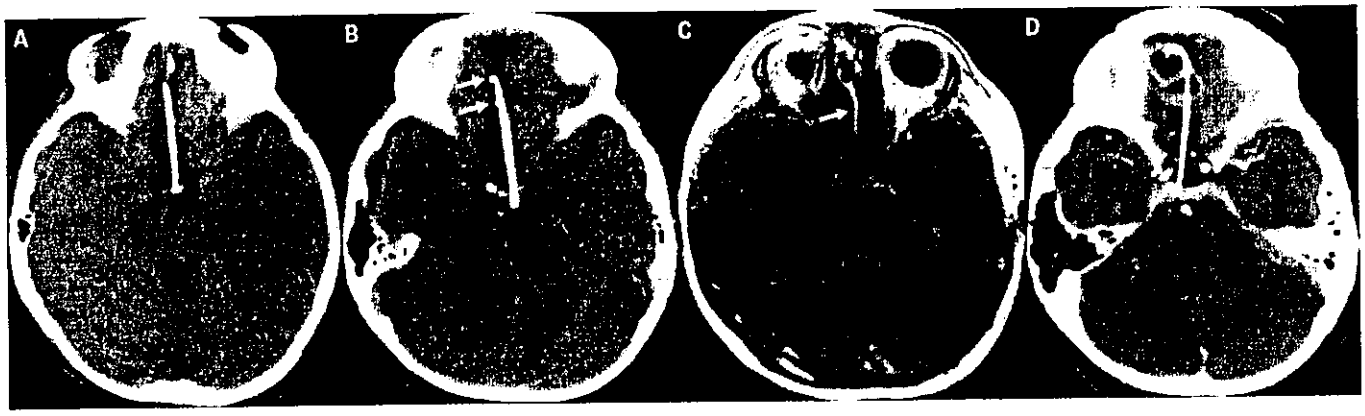

Fig. 4. Plain CT, the day after the previous (second) surgery (**A**), showed total removal of the tumor and no minute calcification around the Ommaya reservoir cannula. However, plain CT, 6 days after the previous (second) surgery (**B**), demonstrated minute calcification around the Ommaya reservoir cannula (white arrows). Axial T_1-weighted gadolinium-enhanced MR images, 2 months after the previous (second) surgery (**C**), demonstrated a cystic mass surrounding the Ommaya reservoir cannula in the center of the frontal base in the subdural space under the craniotomy bone flap. Enhancement along the Ommaya reservoir cannula was noted (white arrow). Enhanced CT, 6 months after the previous (second) surgery (**D**), demonstrated a multilocular cystic mass involving minute calcification surrounding the Ommaya reservoir cannula in the center of the frontal base.

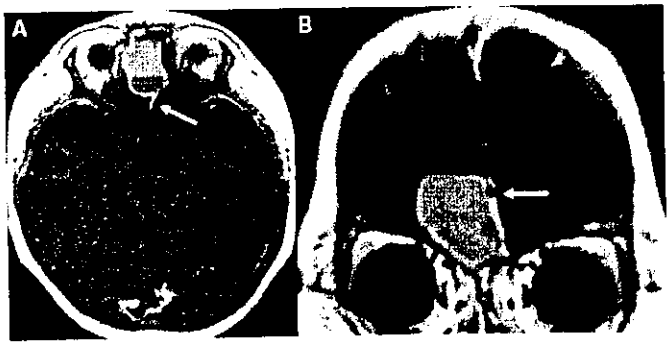

Fig. 5. Axial T_1-weighted gadolinium-enhanced (**A**) and coronal (**B**) MR images, 10 months after the previous (second) surgery, demonstrated a well-enhanced cystic mass. The enhanced lesion followed the Ommaya reservoir cannula. **A** Enhancement along the Ommaya reservoir cannula was noted (white arrow). **B** The wall of the cystic mass involving the cannula (white arrow).

Discussion

The ectopic recurrence of craniopharyngioma is a very rare postoperative complication and, to our knowledge, only 12 such cases have been reported [4–15]. Eight reports in the literature have described ectopic recurrence after the dissemination of residual tumor cells along the tract of the previous surgical route [4, 5, 7, 10–12, 14, 15]. Among these cases was 1 patient with an epidural mass [12] and 2 with masses in the sylvian cistern [10, 14]. In 4 other reports, ectopic recurrence was considered remote metastasis of the primary tumor by cerebrospinal fluid (CSF) dissemination because the site of the recurrent tumor was anatomically separate from both the primary site and the previous surgical route [6, 8, 9, 13]. One of these cases involved the spinal canal [9]. Nomura et al. [13] reported a case that clearly demonstrates CSF dissemination based on positive CSF cytology.

In our case, the ectopic recurrence was considered the dissemination of residual tumor cells along the tract of the previous surgical route, because the recurrent tumor was located along the line of the previous surgical approach. However, it presented unique aspects differing from the 12 previously reported cases. First, this patient was very young: in previous reports, the patients' age at presentation ranged from 10 [4] to 73 years [6], while age was not reported in 1 patient [15]. Second, the time to seeding was very short, only 2 months. In the 12 reported cases, remote recurrence was detected from 20 months [13] to 21 years [12] after the previous surgical intervention. In 1 of these cases, malignant transformation was detected [13]. Third, the tumor recurred along the Ommaya reservoir cannula, surrounding it and grew gradually. Bleyer et al. [16] presented a patient treated for meningeal Burkitt's lymphoma, and the cause of death was a large mass of tumor cells growing around the cannula. These authors considered that Burkitt's cells disseminated along the cannula track deeply into the brain parenchyma. In our case, unfortunately, the Ommaya reservoir cannula was acci-